Massive Stars Near and Far
Proceedings IAU Symposium No. 361, 2024
J. Mackey, J. S. Vink, & N. St-Louis, eds.
doi:10.1017/S1743921322003209

Exploring a direct observational method to measure high-redshift cloud collapse timescales and GRB progenitor lifetimes

Jeff Cooke[1,2,3], Nandita Khetan[4], Sandra Savaglio[5], Jielai Zhang[1,3] and Mark Suhr[1,2]

[1]Centre for Astrophysics and Supercomputing, Swinburne University of Technology, Hawthorn, Victoria 3122, Australia
email: jcooke@astro.swin.edu.au

[2]ARC of Excellence for All Sky Astrophysics in 3 Dimensions *(ASTRO 3D)*

[3]ARC Centre of Excellence for Gravitational Wave Discovery *(OzGrav)*

[4]DARK Cosmology Centre, Niels Bohr Institute, University of Copenhagen, Jagtvej 128, 2200 Copenhagen, Denmark

[5]Department of Physics, University of Calabria, I-87036 Arcavacata di Rende, Italy

Abstract. Long gamma-ray bursts (LGRBs) and superluminous supernovae (SLSNe) are expected to result from massive star deaths. However to date, there has been no direct observational measurement of their cloud collapse timescales nor progenitor lifetimes to help constrain their mass. Our analyses of $z \gtrsim 2$ LGRB afterglow spectra and *Hubble Space Telescope* images find a higher fraction of host galaxies that are interacting, have a close companion, and/or may have experienced a recent galaxy 'fly by' as compared to the general $z \gtrsim 2$ galaxy population. A smaller set of $z \gtrsim 2$ SLSNe suggests a similar result. Under the hypothesis that galaxy interactions induce cloud collapse and star formation near their closest approach, we explore measurements of the host and companion galaxy velocities and separations at the time of the LRGB/SLSN event as a direct physical means to measure the timescale of cloud collapse plus progenitor star lifetime.

Keywords. gamma rays: bursts — galaxies: high-redshift — galaxies: interactions — supernovae: general — stars: evolution — stars: formation

1. Introduction

Galaxy interactions induce star formation, with direct evidence of massive star formation found, for example, by increased emission line strengths from HII regions as a function of separation and observed OB stars in-between interacting galaxies and within tidal tails (e.g., Patton et al. 1997, Barton et al. 2000, Barton Gillespie et al. 2003, de Mello et al. 2008). Under the assumption that long gamma-ray bursts (LGRBs) and superluminous supernovae (SLSNe) result from the deaths of short-lived massive stars, these events would be observed shortly after galaxy interactions. Here, we summarise our analyses to date of high-redshift ($z \gtrsim 2$) LGRB afterglow spectra and *Hubble Space Telescope (HST)* imaging that indicate a large fraction of LGRB host galaxies experiencing recent galaxy interactions. A subset of LGRBs with interacting hosts occur on the outskirts of their host galaxies in-between the host and the companion/interacting galaxy and/or in their tidal tails. We find a similar result for $z > 2$ SLSNe. We hypothesise that these recent galaxy interactions induced star formation that formed the LGRB/SLSN

progenitor stars and that the physical separations of the galaxy pairs, combined with their relative velocities, are a direct physical measure of the timescales for progenitor cloud collapse and lifetimes. Finally, many of such interactions are expected to induce star formation in the outer regions of the host galaxies, which are typically low metallicity environments. This approach, applied to larger datasets, along with deep host and companion galaxy imaging and spectra, may provide an independent means to test for a metallicity preference for LGRB/SLSN progenitor star formation.

2. Data

2.1. *LGRB afterglow spectra*

Our LGRB afterglow spectra sample includes 191 spectra from 245 LGRBs with measured redshifts detected from 1997–2015 compiled by GHostS† (Savaglio et al. 2007). We focus on those at z $\sim$ 2–6 (94 LGRBs) to enable host and companion galaxy UV absorption line detection, including the Lyα feature. Assessment of additional spectra is underway. Of the 94 afterglow spectra, an initial sample of 40 were assessed that have sufficient signal-to-noise ratio (S/N), resolution, and spectral quality for the work discussed here.

2.2. *Host galaxy imaging and spectra*

Morphological assessment of z $>$ 2 galaxies requires space-based imaging resolution. Our initial *HST* imaging sample consists of 54 z $\gtrsim$ 2 LGRB host galaxies with varying quality and depths acquired by various programs and extracted from the Mikulski Archive for Space Telescopes‡. Our z $>$ 2 SLSN *HST* imaging sample is pulled from the Subaru HSC SHIZUKA survey (Moriya et al. 2019) in the COSMOS legacy field and ground-based imaging for SLSN SN2213-1745 (Cooke et al. 2012) from the Canada-France-Hawaii Telescope Legacy Survey (CFHTLS). Spectroscopy of SN2213-1745 and its companion galaxy were obtained 03 September 2010 with the Low-Resolution Imaging Spectrometer (LRIS; Oke et al. 1995, Steidel et al. 2004) mounted on the Keck-I telescope.

3. Analysis

3.1. *Pair absorbers*

A 'pair absorber' is defined here as an LGRB afterglow spectrum exhibiting two sets of galaxy absorption-line features assumed to be the LGRB host galaxy and a galaxy in the line of sight. We find 5/40 afterglow spectra (13%) with pair absorption having velocity separations $<$ 1000 km s^{-1} (Figure 1). We do not include systems with $\lesssim$ 200 km s^{-1} velocity separation, e.g., those with small relative velocities or systems moving roughly tangential to the line of sight, as they are difficult to identify as separate systems in low-resolution spectra or discern from certain host galaxy rotation profile signatures. Thus, the true fraction of systems with line-of-sight pair absorption is $>$ 13%.

3.2. *Geometry*

The geometry of LGRB host galaxies and the occurrence of pair absorption is illustrated in Figure 2. The host galaxy is located in the centre of the sphere and the LGRB is detected by the observer to the left. The radius, r, indicates the radius of interest. A companion galaxy with r $<$ 30 kpc is defined as an imminent merger and a close pair is defined having r $<$ 50 kpc. A companion galaxy behind the LGRB host will not be detected in absorption by the observer. Considering only this aspect, the observed line-of-sight $>$ 13% pair absorption fraction becomes $>$ 26% for randomly oriented systems.

† http://www.grbhosts.org
‡ https://archive.stsci.edu/

https://doi.org/10.1017/S1743921322003209 Published online by Cambridge University Press

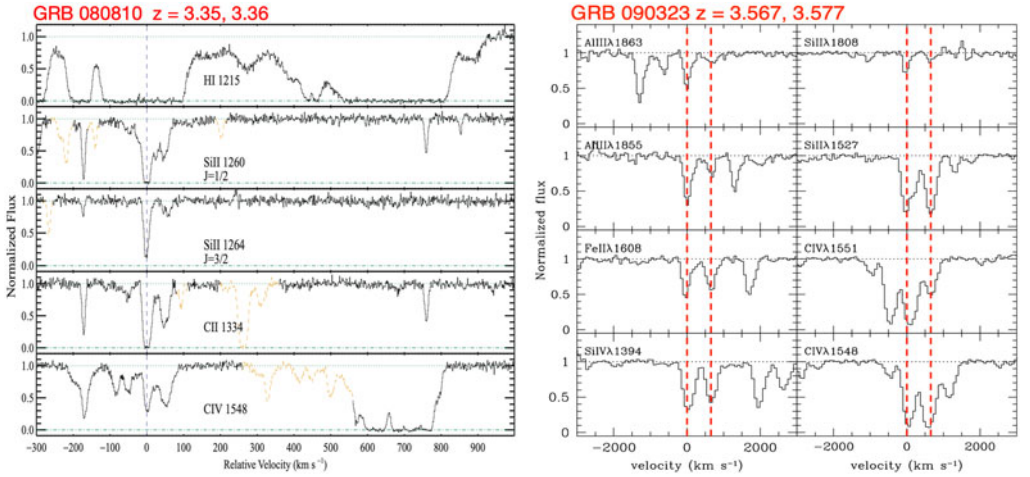

Figure 1. Two example z > 2 LGRB afterglow spectra (Page et al. 2009, Savaglio et al. 2012). The spectra show two sets of galaxy absorption lines, termed pair absorbers, with one set from the host galaxy and the other from a putative companion galaxy.

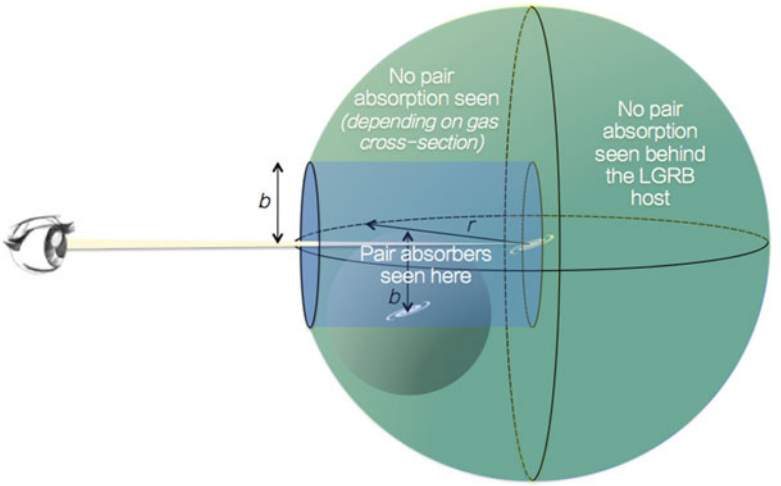

Figure 2. Geometry of an LGRB host galaxy and the ability to observe absorption by a companion galaxy. The LGRB host galaxy is in the centre, the LGRB is seen by the observer to the left, and 'r' indicates the radius of interest for the companion galaxy separation. Companion/interacting galaxies behind the host with respect to the observer are not seen in absorption. Thus, considering random orientations and nothing else, the fraction of pair absorbers observed in LGRB afterglow spectra is > 26% (see § 3.2). The separation between the companion galaxy centroid and the observer's line of sight is indicated by the impact parameter 'b'. The blue region illustrates that only companion galaxies within a cylinder with radius b in LRGB sightlines can be observed as pair absorbers *(see text)*. Using impact parameters from DLA sightlines to QSOs and background galaxies, the fraction of companion galaxies is estimated to be $\gtrsim$ 50%.

The impact parameter, b, is the separation between the LGRB line of sight and the foreground galaxy centroid in which the foreground galaxy absorption is seen in the afterglow spectrum consistent with observations. Thus, a companion galaxy needs to reside within the cylindrical-shaped region (blue in Fig. 2) to appear as a pair absorber.

https://doi.org/10.1017/S1743921322003209 Published online by Cambridge University Press

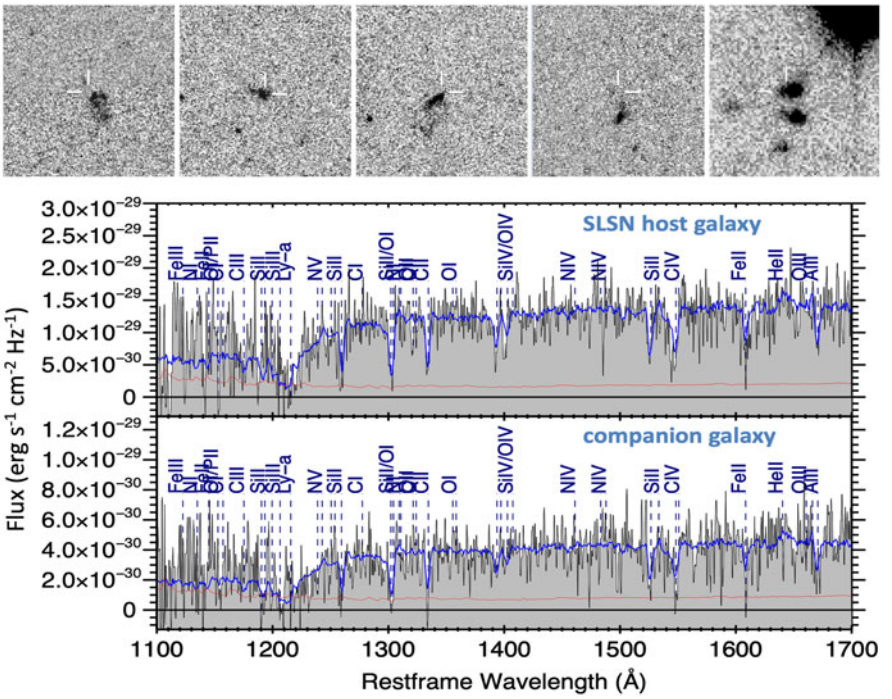

Figure 3. Upper panels: *HST* images of z > 2 SLSN host galaxies with the locations of the SLSNe indicated. Left to right: The first four images are *HST* images (∼7.5 arcsec a side) of HSC17dbpf, z_{spec} = 1.851; HSC16adga, z_{spec} = 2.399; HSC17auzg, z_{spec} = 1.965; HSC16bvv, z_{phot} = 2.5, and the rightmost image is a CFHT Megacam image (15 arcsec on a side) of SN2213-1745, z_{spec} = 2.046 (Curtin et al. 2019, Moriya et al. 2019, Cooke et al. 2012) Lower panels: Keck 1D LRIS spectroscopy of SN2213-1745 host galaxy and companion reveals a ∼150 km s^{-1} velocity difference. The spectrum (black with grey fill) has the positions of high-redshift star forming galaxy far-UV stellar and ISM lines marked by the vertical dashed lines and labelled. A Lyman break galaxy composite spectrum is overlaid (blue curve). The galaxy centroid separation in the image is 21.8 kpc.

Impact parameters for damped Lyman α systems (DLAs) seen in the sightlines to background QSOs and sightlines to background galaxies range from ∼0–25 kpc, as a function of HI column density, i.e., higher column densities have smaller impact parameters (e.g., Krogager et al. 2012, Christensen et al. 2014, Cooke & O'Meara 2015). Using 13% as the observed line-of-sight pair absorber fraction in LGRB afterglow spectra, an impact parameter of ∼21 kpc would correspond to 13% observed coverage (i.e., the fraction residing in the sightline cylinder) if 100% of LGRB host galaxies have interacting or companion galaxies within 50 kpc. Similarly, for host-companion galaxy separations of 30 kpc an impact parameter of ∼13 kpc corresponds to 100% companion fraction. More distant companions or larger impact parameters would correspond to < 100% overall fraction. From the *HST* images, we find that the LGRB host galaxy interactions and close companions have ∼10–20 kpc impact parameters (see Figure 4).

3.3. *Imaging*

An initial assessment of the LGRB *HST* host galaxy images finds 35% displaying interaction features i.e., disturbed morphology, tidal tails and/or mergers (e.g., Figure 4) and an additional 28% host galaxies having close pairs (in projection). A more rigorous assessment of these systems is underway. We note that the *HST* images were not acquired

https://doi.org/10.1017/S1743921322003209 Published online by Cambridge University Press

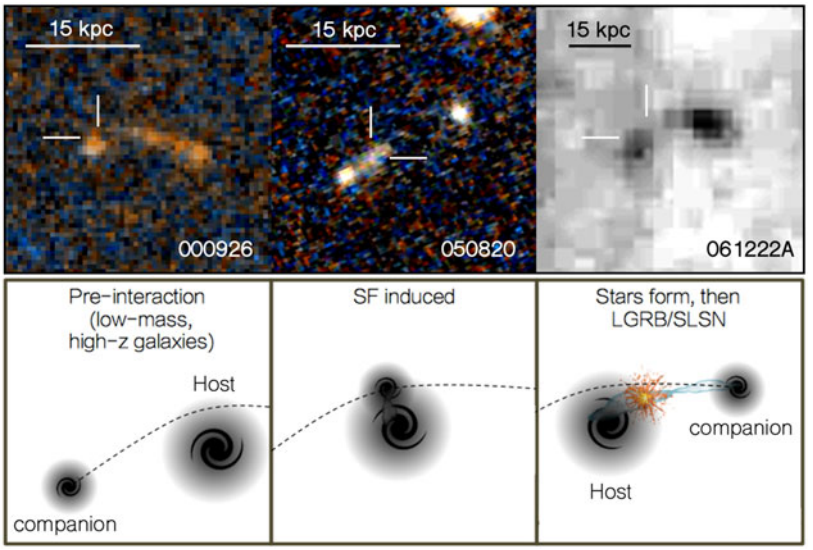

Figure 4. Upper three panels: A subset of LGRBs are found on host galaxy outskirts, in-between the host galaxy and a companion galaxy, and/or along visible tidal tails. Lower three panels: Hypothesis presented in this work. Left: A companion galaxy approaches the LGRB host galaxy. Centre: the companion galaxy interacts with the host, inducing star formation (SF). Right: After some time, the LGRB is observed and the companion has travelled some distance (typically ∼10–20 kpc on the sky). The right panel can be compared to the upper panels of interacting LGRB galaxies. Measuring the time that the companion galaxy would take to travel the physical separation between the two galaxies at the time of the observed LGRB at their velocities, yields the timescale of the induced cloud collapse plus lifetime of the progenitor star.

with the intent to reach sufficient depths to perform a thorough search for close companions, disturbed morphology, or tidal features at these high redshifts. Thus, the number of systems with a faint close companions or evidence of interaction may be higher.

This assessment can be compared to the ∼10–20% merger and close pair fractions for field galaxies at $z > 2$ from observation and simulations (e.g., Conselice et al. 2008, Bertone & Conselice 2009, Berrier & Cooke 2012, Ventou et al. 2019). The ∼10–20% fraction is dependent on host galaxy mass and corresponds to a mass range ($8 < \log M_* < 10$) consistent with those for LGRB host galaxies.

Finally, we include a similar assessment of $z \gtrsim 2$ SLSNe. Figure 3 presents five SLSNe; four with *HST* imaging and one with ground-based CFHTLS imaging. The SLSNe appear to occur on the edge or outskirts of their host galaxies in the *HST* images (without adding projection) and some have signs of interaction or disturbed morphology. The SN2213-1745 host galaxy has a nearby companion and both galaxies appear to show tidal features. The two galaxies are relatively bright and help accommodate 8m-class spectroscopy. We observed the two galaxies 626 days (rest-frame) after the supernova initial detection and the 1D spectra are shown in Figure 3. Both galaxies have the same redshift to within ∼150 km s^{-1} and are separated on the sky by 21.8 kpc. As such, they exhibit a similar behaviour as LGRB galaxies with identified companions or interactions.

4. Discussion

Our initial analyses of LGRB afterglow pair absorbers and *HST* imaging, along with the geometry of the events, indicate that $z > 2$ LGRB host galaxies have a higher interaction and close pair fraction than ∼10–20% found for $z > 2$ galaxies. We find

https://doi.org/10.1017/S1743921322003209 Published online by Cambridge University Press

tentative evidence for a similar result for SLSNe. One reason for the higher fraction is that LGRBs/SLSNe may preferentially point to sites of galaxy interaction with recently induced star formation. Under the assumption that LGRB/SLSN progenitors are massive stars with short lifetimes, the two galaxies involved in the interaction will have only travelled a short distance during the time required for the expected cloud collapse plus progenitor lifetime (i.e., from birth to GRB/SLSN death). For example, galaxies with a relative velocity difference of 500 km s^{-1} would travel ∼10–20 kpc in ∼20–40 Myr.

Interestingly, an LGRB host galaxy subset shows imaging evidence of the above scenario, with ∼10–20 kpc host–companion separations and the LGRB location on the outskirts of their host galaxy or in-between the two galaxies in the tidal tails (Figure 4). Given that these systems are viewed at all orientations in projection, we can estimate that typical real space separations are roughly ∼10–40 kpc, for 0–60° pair inclinations (i.e., to include ∼88% of the ∼10–20 kpc separation cases). If our hypothesis that the LGRB (or SLSN) progenitor star formation is induced by the interaction near closest approach, the time required for each system of two interacting galaxies to reach the measured separation at the time of the observed LGRB (or SLSN) event, travelling at their measured velocities, is a direct measure of the cloud collapse and progenitor star lifetime.

Future deep space-based host galaxy imaging with *HST*, *Euclid*, *Roman*, and *JWST* and deep spectroscopic analysis of their velocities and metallicities with *JWST* and 30m-class telescopes will fully test this hypothesis and, if confirmed, will provide direct measurements of cloud collapse timescales to inform simulations and progenitor mass measurements of LGRBs, and potentially SLSNe, lending deeper insight into their nature.

References

Barton, E. J., Geller, M. J., & Kenyon, S. J. 2000, ApJ, 530, 660
Barton Gillespie, E., Geller, M. J., & Kenyon, S. J. 2003, ApJ, 582, 668
Berrier, J. C. & Cooke, J. 2012, MNRAS, 426, 1647
Bertone, S. & Conselice, C. J. 2009, MNRAS, 396, 2345
Christensen, L., Møller, P., Fynbo, J. P. U., et al. 2014, MNRAS, 445, 225
Conselice, C. J., Rajgor, S., & Myers, R. 2008, MNRAS, 386, 909
Cooke, J., Sullivan, M., Gal-Yam, A., et al. 2012, Nature, 491, 228
Cooke, J. & O'Meara, J. M. 2015, ApJL, 812, L27
Curtin, C., Cooke, J., Moriya, T. J., et al. 2019, ApJS, 241, 17
de Mello, D. F., Smith, L. J., Sabbi, E., et al. 2008, AJ, 135, 548
Krogager, J.-K., Fynbo, J. P. U., Møller, P., et al. 2012, MNRAS, 424, L1
Moriya, T. J., Tanaka, M., Yasuda, N., et al. 2019, ApJS, 241, 16
Oke, J. B., Cohen, J. G., Carr, M., et al. 1995, PASP, 107, 375
Page, K. L., Willingale, R., Bissaldi, E., et al. 2009, MNRAS, 400, 134
Patton, D. R., Pritchet, C. J., Yee, H. K. C., et al. 1997, ApJ, 475, 29
Prochaska, J. X., Neeleman, M., Kanekar, N., et al. 2019, ApJL, 886, L35
Savaglio, S., Budavári, T., Glazebrook, K., et al. 2007, The Messenger, 128, 47
Savaglio, S., Rau, A., Greiner, J., et al. 2012, MNRAS, 420, 627
Steidel, C. C., Shapley, A. E., Pettini, M., et al. 2004, ApJ, 604, 534
Ventou, E., Contini, T., Bouché, N., et al. 2019, A&A, 631, A87

https://doi.org/10.1017/S1743921322003209 Published online by Cambridge University Press